

HERA: Discussion Design

Hydrogen Epoch of Reionization Array

1 Introduction

The Hydrogen Epoch of Reionization Array (HERA) project

This document provide an initial discussion design (aka strawman). It is meant to introduce one plausible system design for discussion. The design is then to be iterated to the point of a first version of a real architecture and design. Figure 1 shows an overall block diagram of the system, identifying the major subsystems, which are discussed below. Note that blocks bordered with dashed lines indicate optional or variational elements.

The design is for about 1000 elements. As discussed below, the elements will likely be aggregated in groups of three at the node and groups of eight in the digital system, so the target number is $3 \times 8 \times 42 = 1008$ elements.

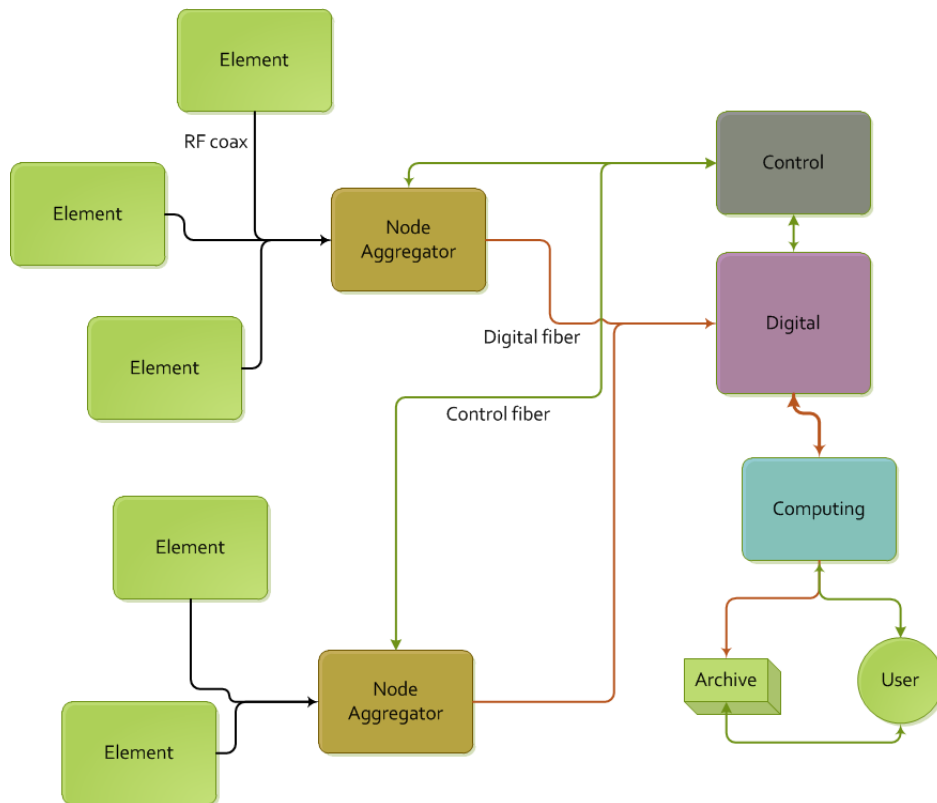


Figure 1: Overall system block diagram.

2 Feed

Desirable features of the antenna feed are:

- bandwidth ~ 1 octave (100-200 MHz)
- evolution of gain versus frequency \ll frequency structure intrinsic to foregrounds
- stability of gain versus time and temperature

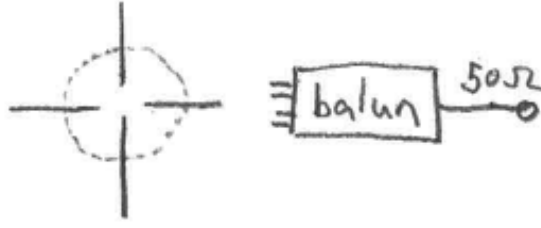


Figure 2: Antenna feed, with active balun. Output is 50Ω coaxial cable for two polarizations.

- matching of polarization beams to minimize polarization leakage
- first-stage amplification with $T_{\text{LNA}} \ll T_{\text{sky}}$. Of order 100 K.

We currently have two feeds that have been field-tested: the PAPER feed and the MWA feed (of which 16 make up an MWA tile). Both designs use linear polarization feeds. These are relatively straight-forward to make, but tend to have significant problems with polarization leakage over wide fields of view.

ISSUES: need for resistor load and/or phase switch at feed?

2.1 PAPER Feed

The PAPER feed is a dual-polarization approximation to a sleeved dipole design that approximately matched to a 100-200 MHz bandwidth. The PAPER feed’s frequency evolution, when paired with a flapped groundscreen that approximates a corner reflector (§3), has been demonstrated to have many of the properties necessary for the delay-spectrum approach to foreground avoidance. PAPER feeds are currently relatively expensive per item, and could benefit from an iteration of design for manufacture.

Although PAPER does reasonably well with 75Ω coaxial cable connecting antenna feeds to receivers, the necessary transition from 75Ω to the 50Ω SMA standard used within the correlator requires an impedance matching network that can easily cause problematic signal reflections. We suggest that it would be better to push the impedance mismatch up to the very front of the system.

2.2 MWA Feed

The MWA feed follows a bowtie design that has a substantially wider operational bandwidth (XXX–300 MHz) than PAPER feeds. It has not yet been demonstrated whether these feeds have the properties necessary for delay-spectrum foreground avoidance. MWA elements have undergone a design for manufacture step, and are relatively inexpensive per item. In particular MWA LNAs are much cheaper (by an order of magnitude) than PAPER baluns.

Has there been any significant study of single MWA feeds (i.e. not part of a beamformed tile)?

3 Element

The element sub-system is meant to maximize the sensitivity with minimal hardware. The design of the element, which integrates a feed (§2) with a reflective structure, is central to both the foreground response of the instrument, and the overall sensitivity.

There is much that we still do not know about the problem of suppressing foregrounds to the 21cm signal from the Epoch of Reionization. Many approaches have been proposed, but without a detection, it is hard to know which approach will ultimately be the most successful. However, there is some convergence around the idea of the foreground “wedge” that represents a baseline-length

dependent threshold for where smooth-spectrum foreground emission can enter an interferometric measurement. Experiments then have a choice of whether to pursue a detection of 21cm EoR emission within the wedge, which requires yet undemonstrated levels of calibration and foreground modeling, or to work outside of the wedge and shoulder more stringent sensitivity requirements.

There are limits to this characterization. Models of the 21cm EoR power spectrum tend to fall off below $k \sim 0.1 h\text{Mpc}^{-1}$, indicating that the sensitivity benefits of working at smaller k do not hold indefinitely. Moreover, there are foregrounds/systematics that arise outside of the wedge (with polarization leakage being most likely the worst) that require a strategy even for experiments working outside of the wedge.

With polarization leakage being one of the biggest concerns that has yet to be addressed, it will be important to provide several pathways to mitigate this potential issue. One important pathway to doing this is in the design of the element itself. The element may restrict the field of view or otherwise compensate for differences in polarization beams so as to mitigate polarization leakage issues. The MWA and PAPER are just on the cusp of being able to study the polarization leakage for these elements. ? predict that without direction-dependent calibration, PAPER leakage will be $\sim 5\%$, and depending on how polarized foregrounds behave, this may cause a systematic bias in measured power spectra of around 1000 mK^2 between $0.2 \leq k \leq 1.0 h\text{Mpc}^{-1}$. One potential approach to mitigating raw polarization leakage is to design elements that do a better job of matching polarization beams. This might be done through apodization (at low frequencies, this might even be done by overilluminating a reflector), or by tailoring a reflector to match beams. PAPER is currently demonstrating how fringe-rate filters can be used to tailor beam responses between declination bins. This may be used to reduce a 2D beam matching problem to a 1D problem.

In general, we propose that HERA adopt a strategy of bringing enough sensitivity on shorter baselines to avoid the necessity of working inside of the wedge for the key EoR science goals, but to provide the “hooks” for the possibility of eventually working within the wedge. In essence, this entails designing elements tailored to a delay-spectrum approach to detecting 21cm EoR, but addressing the needs of imaging, etc., in the array configuration. A key requirement for any element used in 21cm intensity mapping is that resonances and reflections within the element not modulate otherwise spectrally-smooth foreground emission on frequency scales that one might hope to measure the high-redshift 21cm signal.

Desirable features of elements (apart from feeds) are:

- ability to be placed within 30m (or better, 16m) of one another to support the short baselines required by delay-spectrum foreground avoidance
- reflections arising from foreground signals bouncing within the element be attenuated by -60dB for time delays $\tau < 100\text{ns}$
- polarization beams matched to better than 0.5% , or if this is not possible, matched at this level following a reweighting along one axis (i.e. declination contours, as discussed above)
- maximal collecting area (or rather, minimal beam area) given constraints above. As shown in Appendix B of ?, the key sensitivity metric here is $\Omega' = \frac{\Omega_{\text{P}}^2}{\Omega_{\text{PP}}}$
- ruggedness

We currently have three different designs on the table. The PAPER element uses a reflective groundscreen with flaps that approximates a corner reflector for a dipole feed. The MWA element consists of 16 feeds closely packed on a reflective screen. A third design is a parabolic dish approximately 10 m in diameter with a focal length of 3.5 m, statically pointing up.

ISSUES: is spec on polarization leakage attainable? Tracking vs. drift-scanning. Is the spec on reflections attainable for an obstructed aperture such as a parabolic dish?

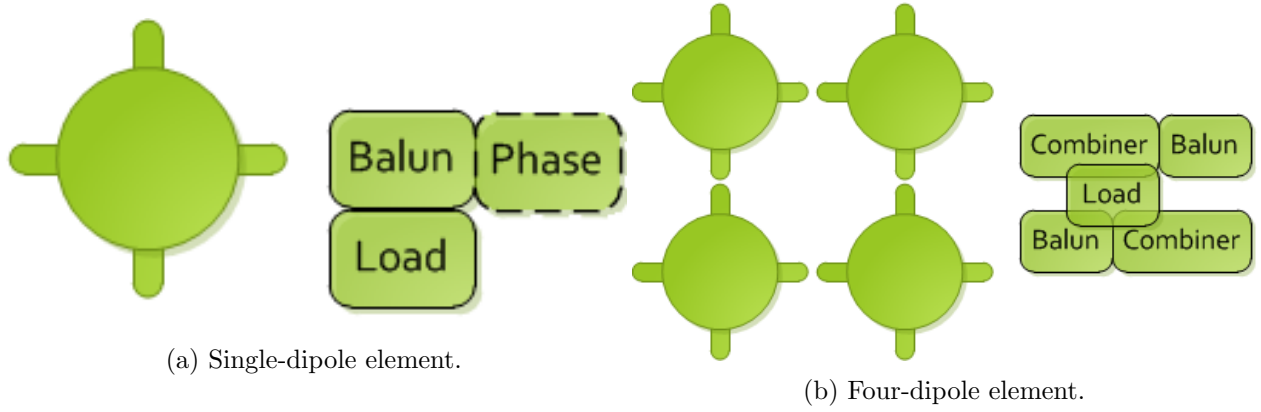


Figure 3: Element configurations.

3.1 PAPER Groundscreen

PAPER groundscreens are currently one of the smallest elements being used for 21cm EoR analysis. This comes at a significant penalty in sensitivity. However, per feed, they nearly maximize collecting area without obstructing the aperture, and have very little capacity for internal reflection, which make them very effective for delay-spectrum analysis. Polarization leakage may be a significant problem for these elements, however. They are great for wide-field imaging.

Estimated area: 8 m^2 . $\Omega' = 2.35 \text{ sr}$.

3.2 MWA Tile

This element concept is best exemplified by the MWA tile design. For tile elements, we assume drift-scan observations using static beamforming. This choice is definitely debatable, but the thinking is that the enhanced sensitivity of multiple beams may be outweighed by the associated complexity and cost of operation and calibration.

The sub-system consists of identical elements that are aggregated at a node. The connection between the two has the following interfaces:

- Two RF cables (50Ω , Type-N)
- DC power (2-conductor #18)
- Ground (1-conductor #18)
- Control (2-conductor #24)

Figure 3 shows two possible layouts of dipoles as well as indicating the accompanying RF hardware possibilities. An optional phase switch is shown, which may also go at the node or be omitted. It is not desired to have at the element since logic or faster switching signals are then needed at that location, however it has the greatest potential performance at that location.

In order to maximize sensitivity for a given size correlator, the dipoles may be combined in a static, zenith beamformer (combiner). Depending on the performance details, the combiner may precede the balun to limit hardware needed.

Estimated area: 16 m^2 . $\Omega' \approx 0.18 \text{ sr}$.

3.2.1 Sparse Tiles

The rationale here is that, although imaging requires that grating sidelobes be suppressed by spacing feeds at $\lambda/2$ intervals, 21cm intensity mapping does not necessarily care. In this case, sub-elements

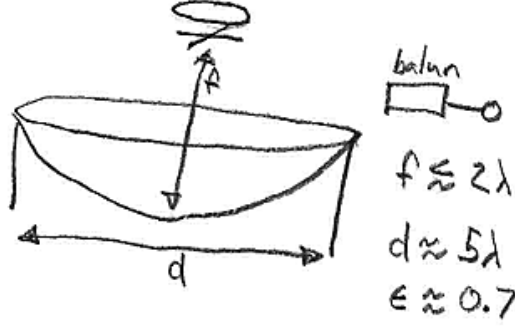


Figure 4

with increased collecting area (think PAPER groundscreens) can be tiled at intervals nearer to λ in length, reducing the number of signal paths at the expense of more infrastructure around each feed. It turns out that the beam metric for tiles peaks at λ spacing. Hence, if we modify the dense tile design above, it is possible to get slightly improved performance.

Estimated collecting area: 22 m^2 . $\Omega' \approx 0.13 \text{ sr}$.

3.3 Parabolic Dish

This element concept is novel, but bears similarities to a drift-scan observing mode explored on the GMRT, and to the cylinder dish concept being explored for CHIME.

In order for a parabolic (or cylindrical) dish to work for 21cm intensity mapping, the focal length and dish diameter must be carefully controlled to avoid reflections that enter at a significant delay, and thus modulate foregrounds to corrupt scales at the corresponding k_{\parallel} . Based on recent work characterizing foregrounds, it seems reasonable to ask that a dish not create more spectral structure than the shortest ($8\lambda \approx 15\text{m}$) baselines that have been shown to be well-behaved. Beyond limiting the dish diameter to 15m, this requirement restricts the focal length, since once of the primary resonances in the dish will be the “narcissistic waves” that arise between the primary and secondary reflector and/or the primary reflector and the antenna feed. These latter waves are a consequence of the necessarily imperfect match of the feed electronics to the impedance of free space.

To mitigate narcissistic reflections, one typically adds an attenuator or “splash cone” directly below the feed. If we posit that reflections must be suppressed by -60dB at delays corresponding to the time it takes to travel 15m, and if we assume that reflections are attenuated by a factor A for each crossing of the attenuator placed below the feed, then the number of allowed reflections, R , is given by

$$R = \text{floor} \left(\frac{-60\text{dB}}{2A} \right). \quad (1)$$

Thus, for a feed height (or focal length), f , we have

$$2Rf < 15\text{m}. \quad (2)$$

For a moderate attenuation value of $A = -15\text{dB}$, we have $f < 4\text{m}$.

As shown in Figure 5, for a chosen focal length of $f = 3.5\text{m}$, dish diameters in the range of 10 to 12m yield efficiencies of $\epsilon \approx 0.7$. Hence, the total effective collecting area of a dish that has been tuned for 21cm intensity mapping at EoR frequencies is of order 80m^2 . The corresponding effective beam area at 150 MHz (noting the issue described in §??) is approximately

$$\Omega' \approx 0.06 \text{ sr}. \quad (3)$$

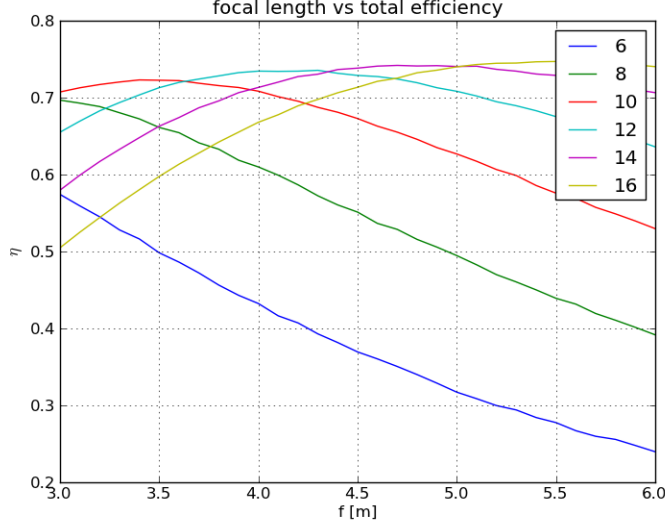


Figure 5: Total efficiency as a function of focal length, for various diameters of parabolic dishes (in meters). Choosing a fiducial focal length of $f = 3.5\text{m}$, dish diameters of $10 \leq d \leq 12\text{m}$ yield efficiencies of $\eta \sim 0.7$.

In addition to the substantial collecting area that this design provides, the relatively narrow field of view associated with a larger dish may go a long way toward mitigating some of the polarization leakage problems that are just on the horizon of being discovered with current designs. However, without concrete measurements, this is largely speculation.

4 Node

A node is responsible for receiving signals from 30 elements, providing secondary amplification, digitizing each signal, and transmitting packetized data over an optical link to a central location (see Figure 6). Nodes are envisioned to be small thermally controlled enclosures that host receiver cards (providing filtering & amplification of RF signals) and digitizers (sampling ≥ 6 RF signals, corresponding to 2 dual-polarization antennas, outputting 10 GbE packetized data via SFP+ ports), along with associated power supplies, cables, sensors, and control systems. There will be 34 nodes in the system (for 1020 elements).

Desirable features in a node are:

- secondary amplification that is a negligible (~ 10 K) source of thermal noise
- thermal and electrical stability
- 100 dB RFI shielding
- better than -40 dB shielding between signal paths

The connection between the node and the the processing facility has the following interfaces:

- one 10 GbE fiber per three elements
- one control fiber pair per node.

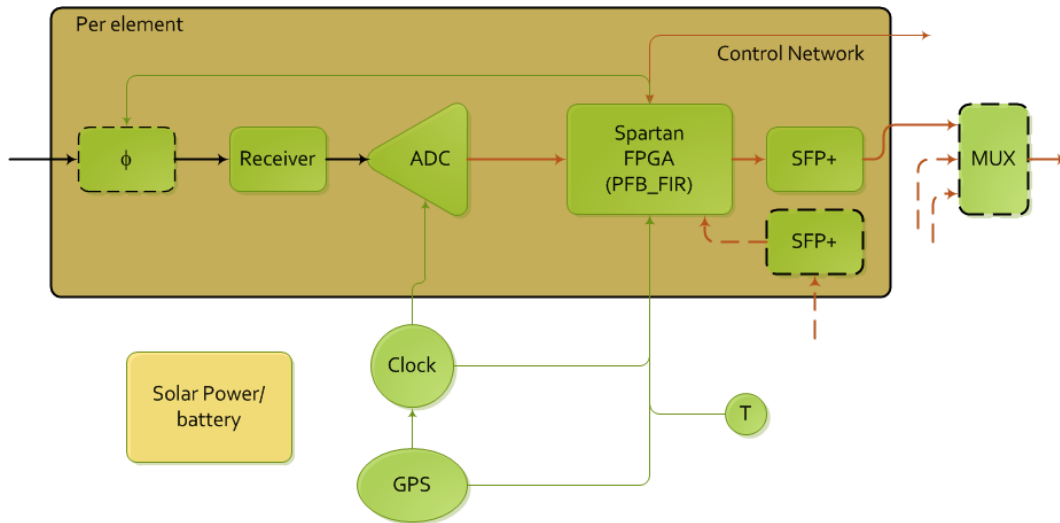


Figure 6: Node configuration.

4.0.1 Receiver

The previously discussed phase switch is shown. The receiver amplifies and filters the signal and the signals are then digitized using the locally-generated clock.

ISSUES: What band should receivers filter to (default: 100-200 MHz)?

4.0.2 Digitizer

One key shortcoming of the current CASPER correlator architecture used for PAPER is that F-engines (currently ROACHs) use connectors to ADC card to import data. As FPGA boards get more powerful, ADCs have to be re-spun to pipe more data into each board. For HERA, we propose to instead digitize in the field and import data over 10GbE to the F engines.

Work is underway to prototype a digitizer board that integrates Hittite ADCs such as those used on CASPER's ADCx16 board with a small Kintex7 FPGA that will be responsible for formatting data into 10 GbE packets to be output over an SFP+ connector. This FPGA will also likely be responsible for implementing a PFB FIR filter, which would require extensive buffering if implemented asynchronously in the digital correlator.

The expected data-rate from each element is $200 \text{ MHz} \times 8 \text{ b} \times 2 \text{ pol} = 3.2 \text{ Gbps}$. A 10 Gb SFP+ optical transducer for 1 km would support three elements to be multiplexed together for transmission back to the processing facility. This multiplexing will likely occur inside the FPGA. This suggests that a node could service factors of three.

A temperature sensor at the node monitoring the external temperature is important for the calibration of the elements. An additional temperature sensor in the node serves as a diagnostic. The node must be cooled for operation and the analog components (including the ADC) should be thermally regulated.

IDEAS: could each node derive its own clock using GPS?

ISSUES: clock distribution. synchronization. is phase switching needed?

5 Digital Correlator

The digital system that comprises a large switch, ROACH2 boards and GPUs and is shown in 7. It should sit within the Karoo Array Processing Building. Note that this will likely be farther than the 1 km limit of the node optical links, so an additional level of aggregation and long-haul

capability will likely be needed (this is discussed later in §7). The capacity for the 1008 system is 3.3 Tbps.

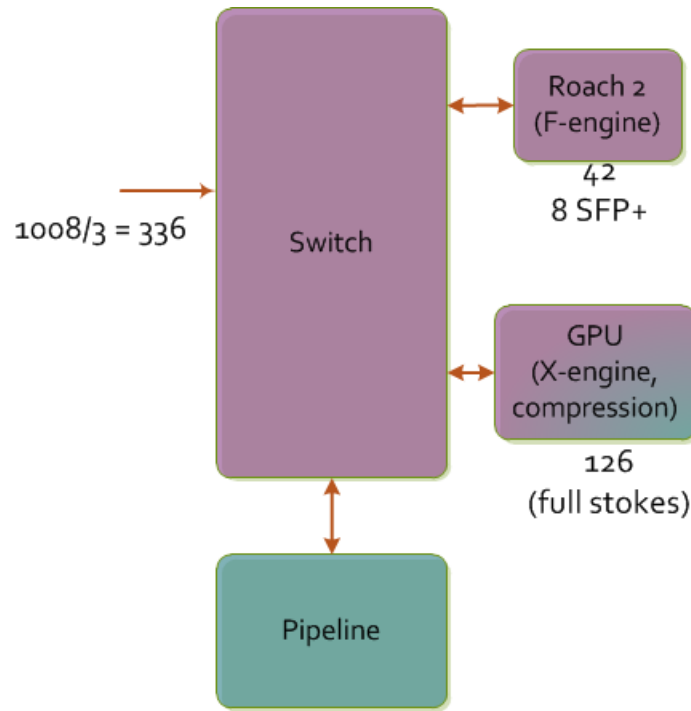


Figure 7: Digital configuration.

The ROACH2 boards will serve as the F-engine for the correlator. Each has 8 bi-directional 10Gb SFP+ connectors. Since at this point there are still 3 antennas per link, there are $1020/3 = 340$ 10GbE inputs. By dropping to 4b+4b real/imag for only positive frequencies, F engines have 1/2 the data output rate. Hence each ROACH2 will need 5 ports reserved for inputting data directly from the field, and 3 reserved for outputting data to the switch used for the correlator corner-turn. Hence $340/5 = 68$ ROACH2 boards are required. It is anticipated that beyond the connectivity, 68 ROACH2 boards will have sufficient compute power to host 15 F engines (a 32-antenna F-Engine design for ROACH2 has already been demonstrated). F Engines will, in total, require 204 switch ports, for an aggregate output rate of 1632 Gbps.

GPUs will serve as X-engines in the correlator (and will also be used to compress data, as discussed in §??). For HERA, we anticipate 2 Moore's Law doublings from currently deployed PAPER technology (the Kepler 690 dual GPU card), allowing a 1024-element full-Stokes correlator to be implemented with 128 GPU boxes, each containing 1 CPU, 2 dual-GPUs, and 1 dual 10GbE NIC. If full Stokes is not needed (i.e. no U,V), the GPU system may possibly be reduced by a factor of 2.

The switch will need $204 + 256 = 460$ ports. If switches this large prove hard to find, an alternate configuration, which may cost a bit more in ROACH2 hardware, could get the total number of switch ports down to 170.

This correlator is anticipated to pull around 100 kW, of which ~95 kW are the GPU boxes. For an observing season, this costs ~\$40 kUSD. Including cooling overhead, that cost rises to ~\$80 kUSD. Although this is within a manageable range, it may be worth examining lower-power alternatives.

For 10-second integrations, the data output rate of the correlator will be 14 Gbps. This is a manageable rate for recording to storage in the short term. However, at 74 TB/day (and 13 PB per campaign), this quickly becomes unwieldy, and a data management plan (did I just say that?) is

required.

ISSUES: power consumption of GPUs is high.

6 Data Management

Given the sheer volume of data output from the correlator, a near-real-time processing system must be in place to reduce data to a manageable volume. A data compression scheme tailored to low-frequency transit telescopes is described in Appendix A of ?. As demonstrated on PAPER, this delay/fringe-rate compression scheme is nearly lossless from the point of view of EoR emission locked to the celestial sphere. Applying the full compression assuming a maximum baseline length of 300m results in a 20x data reduction factor. This reduces the data volume from a campaign (180 days) to 610 TB.

Using benchmarks from deployed PAPER data compression systems, and assuming a 10x speed-up per thread for implementing this compression on GPUs (which preliminary results suggest is reasonable), we anticipate that 64 GPU boxes will be sufficient to compress a 12-hour observation (74 TB) in 8 hours.

Details of the processing/compression, leading to the use of the GPUs during the day to process. This means a 500 TB drive would do the trick.

Data compression is somewhat computationally expensive. However, scaling from currently known run-times on a compute cluster ($64^2/2$ baselines in real time on 2 cores), assuming 2 Moore's Law doublings, and assuming a factor of 10 scaling for computing on GPUs, we get that 205 single GPUs would be sufficient to compress the data. Fortunately, during the daytime, we have 256 dual GPUs available in the correlator. The plan is to use these during the day to compress data.

If we want more flexibility in data analysis, we could temporarily store uncompressed data and then LST bin. This assumes no ionosphere correction, which hasn't been shown to work or be necessary. We can debate this.

We should also have 2PB of tape storage for archiving.

7 Infrastructure

Need some. A lot depends on piggybacking off of other facilities. More to come here.

Operating power: 128 GPU boxes at 1kW, 68 ROACH2 at 200W + 10kW data = 152 kW. Operating for 24 hrs (12 observing + 12 compression) for 300 days = 1.09e6 kWhr. At \$0.10 per kWhr, this is \$110k.